# 130 GeV gamma-ray line and enhancement of $h \to \gamma\gamma$ in the Higgs triplet model plus a scalar dark matter

Lei Wang, Xiao-Fang Han

*Department of Physics, Yantai University, Yantai 264005, China*

## Abstract

With a discrete $Z_2$ symmetry being imposed, we introduce a real singlet scalar $S$ to the Higgs triplet model with the motivation of explaining the tentative evidence for a spectral feature at $E_\gamma$ = 130 GeV in the Fermi LAT data. The model can naturally satisfy the experimental constraints of the dark matter relic density and direct detection data from Xenon100. The doubly charged and one charged scalars can enhance the annihilation cross section of $SS \to \gamma\gamma$ via the one-loop contributions, and give the negligible contributions to the relic density. $< \sigma v >_{SS\to\gamma\gamma}$ for $m_S = 130$ GeV can reach $\mathcal{O}(1) \times 10^{-27} cm^3 s^{-1}$ for the small charged scalar masses and the coupling constant of larger than 1. Besides, this model also predict a second photon peak at 114 GeV from the annihilation $SS \to \gamma Z$, and the cross section is approximately 0.76 times that of $SS \to \gamma\gamma$, which is below the upper limit reported by Fermi LAT. Finally, the light charged scalars can enhance LHC diphoton Higgs rate, and make it to be consistent with the experimental data reported by ATLAS and CMS.

PACS numbers: 12.60.Fr, 95.35.+d, 95.85.Pw, 14.80.Ec

## I. INTRODUCTION

Recently, several groups [1–3] have reported a line spectral feature at $E_\gamma = 130$ GeV in publicly available data from the Fermi Large Area Telescope (LAT) [4]. Moreover, Ref. [3, 5] reported the hints of a second line at around 111 GeV with less statistically significant. The sharp pick of the gamma-ray around 130 GeV can be explained by the 130 GeV dark matter (DM) annihilation into two photons, whose cross section $< \sigma v >_{SS\to\gamma\gamma}$ is $1.27 \pm 0.32^{+0.18}_{-0.28} \times 10^{-27} cm^3 s^{-1}$ ($2.27 \pm 0.57^{+0.32}_{-0.51} \times 10^{-27} cm^3 s^{-1}$) for Einasto (NFW) DM profile employed [1]. Besides, the line at 130 GeV can also be produced by the 142 GeV (155 GeV) DM annihilating to $\gamma Z$ ($\gamma h$ with $h$ being a 125 GeV Higgs boson). The Fermi LAT collaboration takes slightly different search regions and methodology, and sets an upper limit of $< \sigma v >_{SS\to\gamma\gamma} < 1.4 \times 10^{-27} cm^3 s^{-1}$, which is in mild tension with the claimed signal [6].

The cross section of $SS \to \gamma\gamma$ ($1.27 \times 10^{-27} cm^3 s^{-1}$) required by the claimed 130 GeV gamma-ray line signal is approximately 0.042 in units of the thermal relic density value, $< \sigma v >_0 = 3 \times 10^{-26} cm^3 s^{-1}$ [7]. Since the DM is in general electrically neutral, $SS \to \gamma\gamma$ should arise at one-loop through virtual massive charged particles. If the charged particles at the loop are lighter than the DM particle, the corresponding tree-level cross section for annihilations to these charged particles will exceed that of the loop-level process to $\gamma\gamma$ by many orders of magnitude, which conflicts with the the total annihilation cross section to generate the observed relic density. In addition, an enormous annihilation cross section to charged particles is disfavored by the gamma-ray constraints from observations of the Galactic Center and elsewhere [6, 8]. A variety of DM models have been proposed to solve this issue [9–11]. Ref. [9] shows a multi-charged and colored scalar $X$ can enhance $< \sigma v >_{SS\to\gamma\gamma}$ to $\mathcal{O}(1) \times 10^{-27} cm^3 s^{-1}$ via the interaction of $\lambda_X SSXX$ at one-loop, and not lead to the conflict with the relic density for its mass is larger than that of DM. In addition, the LHC diphoton Higgs rate is also enhanced by the scalar.

To construct the DM models economically, a real singlet scalar is respectively added to the standard model [12] and two Higgs doublet model [13] with a discrete $Z_2$ symmetry being imposed. These models can satisfy naturally the constraints from the DM relic density and direct detection data, but hardly accommodate the claimed 130 GeV gamma-ray line signal [14, 15]. In this paper, we introduce such a scalar $S$ to the Higgs triplet model (HTM) which contains a complex doublet Higgs field and a complex triplet Higgs field with

hypercharge $Y = 2$ [16]. In the original HTM, several physical Higgs bosons remain after the spontaneous symmetry breaking, including two CP-even ($h$ and $H$), one CP-odd ($A$), one charged ($H^{\pm}$) and one doubly charged Higgs scalars ($H^{\pm\pm}$). The charged scalars $H^{\pm\pm}$ and $H^{\pm}$ can enhance the cross section of $SS \to \gamma\gamma$ at one-loop. Besides, the SM-like Higgs decay into two photon can be enhanced by these charged scalars, which is favored by the new ATLAS and CMS data. The new Higgs data has been discussed in the HTM [17–19], the minimal supersymmetric standard model (MSSM) [20], the next-to-MSSM [21], and other extensions of Higgs models [22].

This work is organized as follows. In Sec. II, we introduce a real single scalar DM to the Higgs triplet model. In Sec. II, we study the constraints of DM relic density and direct detection data. In Sec. III, we calculate the cross sections of $< \sigma v >_{SS\to\gamma\gamma}$ and $< \sigma v >_{SS\to\gamma Z}$. In Sec. IV, we discuss the enhancement of LHC diphoton Higgs rate. Finally, we give our conclusion in Sec. V.

## II. THE HIGGS TRIPLET MODEL PLUS A SCALAR DM (HTMD)

In the HTM [16], a complex $\mathrm{SU(2)_L}$ triplet scalar field $\Delta$ with $\mathrm{Y} = 2$ is added to the SM Lagrangian in addition to the doublet field $\Phi$. These fields can be written as

$$\Delta = \begin{pmatrix} \delta^+/\sqrt{2} & \delta^{++} \\ \delta^0 & -\delta^+/\sqrt{2} \end{pmatrix}, \qquad \Phi = \begin{pmatrix} \phi^+ \\ \phi^0 \end{pmatrix}. \tag{1}$$

The renormalizable scalar potential can be written as [23]

$$\begin{aligned} V &= -m_\Phi^2 \Phi^\dagger\Phi + \frac{\lambda}{4}(\Phi^\dagger\Phi)^2 + M_\Delta^2 Tr(\Delta^\dagger\Delta) + \lambda_1(\Phi^\dagger\Phi)Tr(\Delta^\dagger\Delta) \\ &+ \lambda_2(Tr\Delta^\dagger\Delta)^2 + \lambda_3 Tr(\Delta^\dagger\Delta)^2 + \lambda_4\Phi^\dagger\Delta\Delta^\dagger\Phi + [\mu(\Phi^T i\tau_2\Delta^\dagger\Phi) + h.c.]. \end{aligned} \tag{2}$$

The Higgs doublet and triplet field can acquire vacuum expectation values

$$\langle\Phi\rangle = \frac{1}{\sqrt{2}}\begin{pmatrix} 0 \\ v_d \end{pmatrix}, \qquad \langle\Delta\rangle = \frac{1}{\sqrt{2}}\begin{pmatrix} 0 & 0 \\ v_t & 0 \end{pmatrix} \tag{3}$$

with $v_{SM}^2 = v_d^2 + 4v_t^2 \approx (246\ \mathrm{GeV})^2$.

After the spontaneous symmetry breaking, the Lagrangian of Eq. (2) predicts the seven physical Higgs bosons, including two CP-even ($h$ and $H$), one CP-odd ($A$), one charged ($H^{\pm}$) and one doubly charged Higgs scalars ($H^{\pm\pm}$). These mass eigenstates are in general

mixtures of the doublet and triplet fields. The experimental value of the $\rho$ parameter requires $v_t^2/v_d^2$ to be much smaller than unity at tree-level, which gives a upper bound of $v_t < 8$ GeV. [17, 24]. For a very small $v_t$, the mixing angle in the CP-even sector $\alpha$ and charged Higgs sector $\beta$ are approximately,

$$\sin\alpha \simeq 2v_t/v_d, \qquad \sin\beta \simeq \sqrt{2}v_t/v_d, \tag{4}$$

and the mixing of the doublet and triplet fields is nearly absent. For this case, the seven Higgs masses can be obtained from the Lagrangian of Eq. (2) [17, 18],

$$\begin{aligned}
m_h^2 &\simeq \frac{\lambda}{2}v_d^2, \\
m_H^2 &\simeq M_\Delta^2 + (\frac{\lambda_1}{2}+\frac{\lambda_4}{2})v_d^2 + 3(\lambda_2+\lambda_3)v_t^2, \\
m_A^2 &\simeq M_\Delta^2 + (\frac{\lambda_1}{2}+\frac{\lambda_4}{2})v_d^2 + (\lambda_2+\lambda_3)v_t^2, \\
m_{H^\pm}^2 &= M_\Delta^2 + (\frac{\lambda_1}{2}+\frac{\lambda_4}{4})v_d^2 + (\lambda_2+\sqrt{2}\lambda_3)v_t^2, \\
m_{H^{\pm\pm}}^2 &= M_\Delta^2 + \frac{\lambda_1}{2}v_d^2 + \lambda_2 v_t^2.
\end{aligned} \tag{5}$$

In the following discussions, we always assume the value of $v_t$ is very small. We take $h$ as the 125 GeV SM-like Higgs boson, which is from the Higgs doublet field. $H$, $A$, $H^\pm$ and $H^{\pm\pm}$ are heavier than $h$, which are from the Higgs triplet field. The $h$ field couplings to $f\bar{f}$, $WW$ and $ZZ$ equal to those of SM nearly. In addition, the scalar potential terms in Eq. (2) contain the SM-like Higgs boson coupling to the charged scalars [18],

$$g_{hH^{++}H^{--}} \approx -\lambda_1 v_d, \qquad g_{hH^+H^-} \approx -(\lambda_1+\frac{\lambda_4}{2})v_d. \tag{6}$$

However, the similar couplings for $H$ are suppressed by the factor $\sin\alpha$, $v_t$ or $\sin\beta$. Thus, the $H$ production cross section at the collider is very small, which satisfies the constraints of the present Higgs data easily.

Now we introduce the renormalizable Lagrangian of the real single scalar $S$,

$$\mathcal{L}_S = \frac{1}{2}\partial^\mu S\partial_\mu S - \frac{m_0^2}{2}SS - \frac{\kappa_1}{2}\Phi^\dagger\Phi SS - \kappa_2 Tr(\Delta^\dagger\Delta)SS - \frac{\kappa_s}{4}S^4. \tag{7}$$

The linear and cubic terms of the scalar S are forbidden by the $Z_2$ symmetry $S \to -S$. $S$ has a vanishing vacuum expectation value which ensures the DM candidate $S$ stable. $\kappa_s$ is the coupling constant of the DM self-interaction, which does not give the contributions

to the DM annihilation and Higgs signal. In order to explain the 130 GeV gamma-ray line, we take DM mass as 130 GeV, which determines the value of $m_0$ by the relation of $m_S = (m_0^2 + \frac{1}{2}\kappa_1 v_d^2 + \kappa_2 v_t^2)^{1/2}$. The total DM annihilation cross sections mainly depend on the $\kappa_1$, which determines the couplings $hSS$ and $hhSS$. $\kappa_2$ determines the couplings $HSS$, $HHSS$, $AASS$, $H^{\pm}H^{\mp}SS$ and $H^{\pm\pm}H^{\mp\mp}SS$, where the coupling $HSS$ is suppressed by $v_t$. The couplings $H^{\pm}H^{\mp}SS$ and $H^{\pm\pm}H^{\mp\mp}SS$ give the important contributions to $XX \to \gamma\gamma$ at one-loop.

For $v_t < 10^{-4}$ GeV, $H^{\pm\pm} \to \ell^{\pm}\ell^{\pm}$ is the dominant decay mode of $H^{\pm\pm}$. Assuming $Br(H^{\pm\pm} \to \ell^{\pm}\ell^{\pm}) = 1$, CMS presents the low bound 383 GeV on $m_{H^{\pm\pm}}$ from the searches for $H^{\pm\pm} \to \ell^{\pm}\ell^{\pm}$ via $q\bar{q} \to H^{\pm\pm}H^{\mp\mp}$ and $q\bar{q} \to H^{\pm\pm}H^{\mp}$ production processes [25]. However, $H^{\pm\pm} \to W^{\pm}W^{\pm}$ and $H^{\pm\pm} \to H^{\pm}W^{*}$ are the dominant modes for $v_t > 10^{-4}$ GeV [17, 18, 26], for which there have been no direct searches. Therefore, the above bound on $m_{H^{\pm\pm}}$ can not be applied to the case of $v_t > 10^{-4}$ GeV, and $H^{\pm\pm}$ could be much lighter in this scenario. In this paper, we take $v_t = 0.1$ GeV and $m_{H^{\pm\pm}}$ to be as low as 140 GeV. LEP searches for the charged scalar give the constraints on the possible existence of light scalars [27]. A conservative lower bound on $m_{H^{\pm}}$ should be larger than 100 GeV due to the absence of non-SM events at LEP. To simplify the parameter space, we take the triplet scalars to be degenerate, namely $\lambda_4 = 0$. We can neglect the contributions of $\lambda_2$ and $\lambda_3$ to the triplet masses which are suppressed by $v_t^2$.

## III. DARK MATTER RELIC DENSITY AND DIRECT DETECTION

### A. calculation of relic density

The degeneracy masses of the triplet scalars are taken to be larger than 140 GeV. Thus, the annihilation processes $SS \to HH,\ AA,\ H^{\pm}H^{\mp},\ H^{\pm\pm}H^{\mp\mp}$ are forbidden for $m_S$ =130 GeV. When the triplet scalars masses are slightly larger than DM mass, the cross section of the forbidden annihilation channel is important [28]. Here, we do not consider this scenario. Since the $H$ field couplings to $SS$, $f\bar{f}$, $WW$, $ZZ$ are suppressed by $v_t$ or $\sin\alpha$, the s-channel annihilation processes mediated by $H$ give a negligible contributions to total DM annihilation cross sections. Therefore, the main annihilation processes include $SS \to f\bar{f}$, $SS \to WW$, $SS \to ZZ$ which proceed via an s-channel $h$ exchange, and $SS \to hh$ which proceeds via a

4-point contact interaction, an s-channel $h$ exchange and t- and u-channel $S$ exchange. The total annihilation cross sections time the relative velocity $v$ for these processes are given as [29],

$$\sigma v = \sigma_{ff} v + \sigma_{WW} v + \sigma_{ZZ} v + \sigma_{hh} v, \tag{8}$$

$$\begin{aligned}
\sigma_{ff} v &= \sum_f \frac{\kappa_1^2}{4\pi} \frac{m_f^2}{(s-m_h^2)^2} (1 - \frac{4m_f^2}{s})^{3/2}, \\
\sigma_{WW} v &= \frac{\kappa_1^2}{8\pi} \frac{s}{(s-m_h^2)^2} \sqrt{1 - \frac{4m_W^2}{s}} \left(1 - \frac{4m_W^2}{s} + \frac{12 m_W^4}{s^2}\right), \\
\sigma_{ZZ} v &= \frac{\kappa_1^2}{16\pi} \frac{s}{(s-m_h^2)^2} \sqrt{1 - \frac{4m_Z^2}{s}} \left(1 - \frac{4m_Z^2}{s} + \frac{12 m_Z^4}{s^2}\right), \\
\sigma_{hh} v &= \frac{\kappa_1^2}{16\pi s} \sqrt{1 - \frac{4m_h^2}{s}} \left[ \left( \frac{s+2m_h^2}{s-m_h^2} \right)^2 - \frac{8\kappa_1 v^2}{s-2m_h^2} \frac{s+2m_h^2}{s-m_h^2} F(\xi) \right. \\
&\quad \left. + \frac{8\kappa_1^2 v^4}{(s-2m_h^2)^2} \left( \frac{1}{1-\xi^2} + F(\xi) \right) \right].
\end{aligned} \tag{9}$$

where $F(\xi) \equiv \text{arctanh}(\xi)/\xi$ with $\xi \equiv \sqrt{(s-4m_h^2)(s-4m_D^2)}/(s-2m_h^2)$, and $s$ is the squared center-of-mass energy.

The thermally averaged annihilation cross section times the relative velocity, $< \sigma v >$, is well approximated by a non-relativistic expansion,

$$< \sigma v > = a + b < v^2 > + \mathcal{O}(< v^4 >) \simeq a + 6b \frac{T}{m_S} \tag{10}$$

The freeze-out temperature $T_f$ is defined by solving the following equation [30],

$$x_f = \ln \frac{0.038 g m_{pl} m_S < \sigma v >}{g_*^{1/2} x_f^{1/2}}. \tag{11}$$

Where $x_f = \frac{m_S}{T_f}$ and $m_{pl} = 1.22 \times 10^{19}$ GeV. $g_*$ is the total number of effectively relativistic degrees of freedom at the time of freeze-out [31]. $g = 1$ is the internal degrees of freedom for the scalar DM $S$. The present-day abundance of $S$ is approximately [30]

$$\Omega h^2 \simeq \frac{1.07 \times 10^{19}}{m_{pl}} \frac{x_f}{\sqrt{g_*}} \frac{1}{(a + 3b/x_f)}. \tag{12}$$

The relic density from the WMAP 7-year result [32] is

$$\Omega_{DM} h^2 = 0.1123 \pm 0.0035. \tag{13}$$

### B. Calculation of the spin-independent cross section between $S$ and nucleon

The results of DM-nucleus elastic scattering experiments are presented in the form of a normalized DM-nucleon scattering cross section in the spin-independent case. In the HTMD, the elastic scattering of $S$ on a nucleon receives the dominant contributions from the $h$ exchange diagrams, which is given as [33],

$$\sigma^{SI}_{Sp(n)} = \frac{m^2_{p(n)}}{4\pi \left(m_S + m_{p(n)}\right)^2} \left[f^{p(n)}\right]^2, \tag{14}$$

where

$$f^{p(n)} = \sum_{q=u,d,s} f^{p(n)}_{T_q} \mathcal{C}_{Sq} \frac{m_{p(n)}}{m_q} + \frac{2}{27} f^{p(n)}_{T_g} \sum_{q=c,b,t} \mathcal{C}_{Sq} \frac{m_{p(n)}}{m_q}, \tag{15}$$

with $\mathcal{C}_{Sq} = \frac{\kappa_1 m_q}{m_h^2}$ [34],

$$\begin{aligned} &f^{(p)}_{T_u} \approx 0.020, \quad f^{(p)}_{T_d} \approx 0.026, \quad f^{(p)}_{T_s} \approx 0.118, \quad f^{(p)}_{T_g} \approx 0.836, \\ &f^{(n)}_{T_u} \approx 0.014, \quad f^{(n)}_{T_d} \approx 0.036, \quad f^{(n)}_{T_s} \approx 0.118, \quad f^{(n)}_{T_g} \approx 0.832. \end{aligned} \tag{16}$$

In fact, here $\sigma^{SI}_{Sp} \approx \sigma^{SI}_{Sn}$. The recent data on direct DM search from Xenon100 put the most stringent constraint on the cross section [35].

### C. results and discussions

In our calculations, $m_S = 130$ GeV and $m_h = 125$ GeV are fixed. Thus, both the relic density and the spin-independent cross section between $S$ and the nucleon are only sensitive to the parameter $\kappa_1$. In Fig. 1, we plot $\Omega h^2$ and $\sigma^{SI}_{Sn}$ versus the $\kappa_1$, respectively. The left panel of Fig. 1 shows that $\kappa_1$ should be around 0.04 to get the correct DM relic abundance. For such value of $\kappa_1$, the right panel shows that $\sigma^{SI}_{Sn}$ is around $1.2 \times 10^{-45} cm^2$, which is below the upper bound presented by Xenon100 data and accessible at the future Xenon1T.

## IV. GAMMA-RAY LINES FROM $SS \to \gamma\gamma$ AND $SS \to \gamma Z$

### A. 130 GeV gamma-ray line from $SS \to \gamma\gamma$

The annihilation $SS \to \gamma\gamma$ may be radiatively induced by massive charged particles in the loop. The charged scalars $H^{\pm\pm}$ and $H^{\pm}$ can give the dominant contributions to

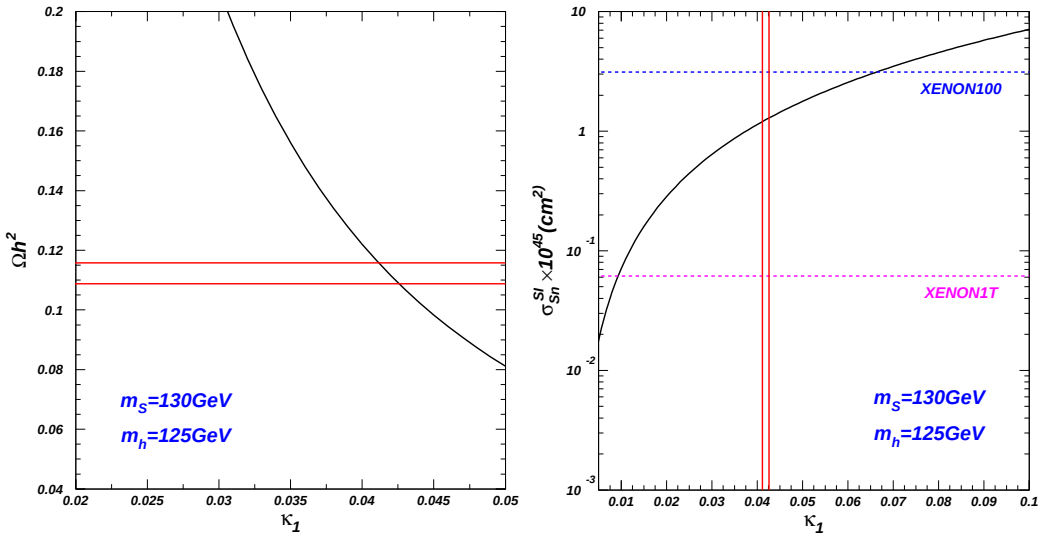


FIG. 1: Left panel: The dark matter relic density versus $\kappa_1$. The horizontal lines show the corresponding bounds from experimental data of the WMAP 7-year. Right panel: the spin-independent cross section between $S$ and the nucleon versus $\kappa_1$. The horizontal lines show the upper bound from Xenon100 and the sensitivity of projected Xenon1T. The vertical lines show the range of $\kappa_1$ constrained by relic density.

this annihilation process via the couplings $H^{\pm\pm}H^{\mp\mp}SS$ and $H^{\pm}H^{\mp}SS$, and the relevant Feynman diagrams are depicted in Fig. 2. Besides, there is another type Feynman diagram for $SS \to \gamma\gamma$ in which s-channel $h$ or $H$ exchange is combined with a charged particle loop. The contributions of the diagram can be sizably enhanced for $m_h$ ($m_H$) $\sim 2m_S$ =260 GeV and the charged particle with an around 130 GeV mass [10]. For the SM-like Higgs $h$, its mass is 125 GeV and the relic density requires $\kappa_1$ to be around 0.04, which suppresses the coupling $hSS$. Although we may take $m_H$ =260 GeV, the coupling $HSS$ is suppressed by $v_t$. Therefore, the contributions from the type diagram are negligible compared to those of Fig. 2. The annihilation cross section corresponding to the diagrams of Fig. 2 is approximately given by

$$< \sigma v >_{SS\to\gamma\gamma} \simeq \frac{\alpha^2\kappa_2^2}{32\pi^3 m_S^2}\left|4E(\tau_{H^{\pm\pm}}) + E(\tau_{H^{\pm}})\right|^2 = \frac{25\alpha^2\kappa_2^2}{32\pi^3 m_S^2}E(\tau_{H^{\pm\pm}})^2 \qquad (17)$$

with $\tau_{H^{\pm\pm}} = \frac{m^2_{H^{\pm\pm}}}{m_S^2}$, $\tau_{H^{\pm}} = \frac{m^2_{H^{\pm}}}{m_S^2}$, and $E(\tau) = 1 - \tau[\sin^{-1}(1/\sqrt{\tau})]^2$. For the second equation, we take $m_{H^{\pm\pm}} = m_{H^{\pm}}$.

The $H^{\pm}$ and $H^{\pm\pm}$ contributions are constructive each other. Because $H^{\pm\pm}$ has an electric

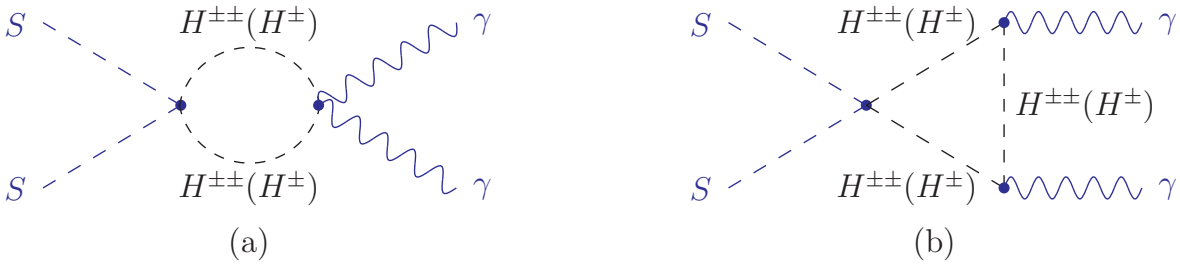


FIG. 2: The Feynman diagrams for $SS \to \gamma\gamma$, which give the dominant contributions to the annihilation process.

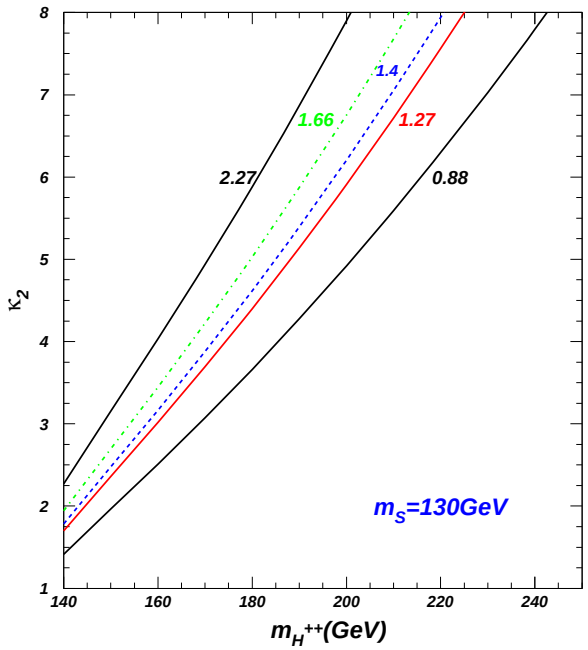


FIG. 3: The contours for $< \sigma v >_{SS\to\gamma\gamma}$ in the plane of $\kappa_2$ versus $m_{H^{\pm\pm}}$. The numbers on the cures denote $< \sigma v >_{SS\to\gamma\gamma} /1.0 \times 10^{-27} cm^3 s^{-1}$.

charge of $\pm 2$, the $H^{\pm\pm}$ contributions are enhanced by a relative factor 4 in the amplitude. Fig. 3 shows some contours for $< \sigma v >_{SS\to\gamma\gamma}= 0.88\times 10^{-27} cm^3 s^{-1}$, $1.27\times 10^{-27} cm^3 s^{-1}$, $1.4\times 10^{-27} cm^3 s^{-1}$, $1.66 \times 10^{-27} cm^3 s^{-1}$, and $2.27 \times 10^{-27} cm^3 s^{-1}$ in the plane of $\kappa_2$ versus $m_{H^{\pm\pm}}$. From Fig. 3, we find that, in order to obtain $< \sigma v >_{SS\to\gamma\gamma}= 1.27 \times 10^{-27} cm^3 s^{-1}$, the minimal value of $\kappa_2$ should be from 1.7 to 4.0 for $m_{H^{\pm\pm}}$ in the range of 140 GeV and 180 GeV. As the increasing of $m_{H^{\pm\pm}}$, the corresponding $\kappa_2$ are required to increase, which will be constrained by the perturbation of the theory.

### B. 114 GeV gamma-ray line from $SS \to \gamma Z$

We can obtain the Feynman diagrams of $SS \to \gamma Z$ and $SS \to \gamma h$ by replacing a $\gamma$ with $Z$ and $h$ in the Fig. 2, respectively. The cross section of $SS \to \gamma h$ is zero due to the charge-conjugation invariance of the interactions involved. The cross section of $SS \to \gamma Z$ is related to that of $SS \to \gamma\gamma$, which is approximately given by

$$\frac{< \sigma v >_{SS\to\gamma Z}}{< \sigma v >_{SS\to\gamma\gamma}} \simeq 2(cot2\theta_W)^2(1-\frac{m_Z^2}{4m_S^2})^{1/2} = 0.76 \tag{18}$$

The energy of this single photon is given by $E_\gamma = m_S(1-\frac{m_Z^2}{4m_S^2}) = 114$ GeV. The current Fermi LAT upper limit on $< \sigma v >_{SS\to\gamma Z}$ for $E_\gamma = 110$ GeV is $2.6\times10^{-27}cm^3s^{-1}$ ($3.6\times10^{-27}cm^3s^{-1}$ ) for Einasto (NFW) DM profile employed [6]. For $< \sigma v >_{SS\to\gamma\gamma}= 1.27\times10^{-27}cm^3s^{-1}$, the prediction value of $< \sigma v >_{SS\to\gamma Z}$ is below the upper bound presented by Fermi LAT.

## V. LHC DIPHOTON HIGGS RATE

To some extent, the $h \to \gamma\gamma$ decay is related to the $SS \to \gamma\gamma$ annihilation, since the doubly charged and one charged scalars can contribute to both $SS \to \gamma\gamma$ and $h \to \gamma\gamma$. It is necessary to restudy the LHC diphoton Higgs rate although it has been studied in detail [17, 18].

Since the new scalars and DM are heavy than the SM-like Higgs $h$, $h$ does not have any new important decay modes compared to that of SM. Except for the decay $h \to \gamma\gamma$, the decay modes and their widths of $h$ are nearly the same both in HTMD and SM. The decay width of $h \to \gamma\gamma$ is expressed as [36]

$$\Gamma(h\to\gamma\gamma) = \frac{\alpha^2 m_h^3}{256\pi^3 v^2}\left|F_1(\tau_W) + \sum_i N_{cf}Q_f^2 F_{1/2}(\tau_f) + g_{_{H^\pm}}F_0(\tau_{H^\pm}) + 4g_{_{H^{\pm\pm}}}F_0(\tau_{H^{\pm\pm}})\right|^2, \tag{19}$$

where

$$\begin{aligned} &\tau_W = \frac{4m_W^2}{m_h^2}, \quad \tau_f = \frac{4m_f^2}{m_h^2}, \quad \tau_{H^\pm} = \frac{4m_{H^\pm}^2}{m_h^2}, \quad \tau_{H^{\pm\pm}} = \frac{4m_{H^{\pm\pm}}^2}{m_h^2}, \\ &g_{_{H^\pm}} = -\frac{v}{2m_{H^\pm}^2}g_{hH^+H^-}, \quad g_{_{H^{\pm\pm}}} = -\frac{v}{2m_{H^{\pm\pm}}^2}g_{hH^{++}H^{--}}. \end{aligned} \tag{20}$$

$N_{cf}$, $Q_f$ are the color factor and the electric charge respectively for fermion $f$ running in the loop. The dimensionless loop factors for particles of spin given in the subscript are:

$$F_1 = 2+3\tau+3\tau(2-\tau)f(\tau), \quad F_{1/2} = -2\tau[1+(1-\tau)f(\tau)], \quad F_0 = \tau[1-\tau f(\tau)], \tag{21}$$

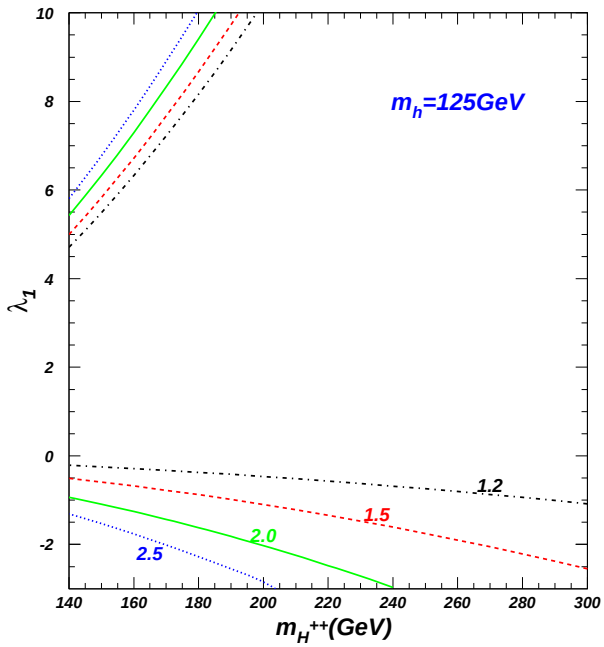


FIG. 4: The contours for $R_{\gamma\gamma}$ in the plane of $\lambda_1$ versus $m_{H^{\pm\pm}}$. The numbers on the cures denote the values of $R_{\gamma\gamma}$.

with

$$f(\tau) = \begin{cases} [\sin^{-1}(1/\sqrt{\tau})]^2, & \tau \geq 1 \\ -\frac{1}{4}[\ln(\eta_+/\eta_-) - i\pi]^2, & \tau < 1 \end{cases} \tag{22}$$

where $\eta_\pm = 1 \pm \sqrt{1-\tau}$.

The Higgs boson production cross section at the LHC are the same both in the HTMD and SM. Therefore, the LHC diphoton rate of Higgs boson in the HTMD normalized to the SM prediction can be written as

$$R_{\gamma\gamma} = \frac{Br(h \to \gamma\gamma)}{Br(h \to \gamma\gamma)^{SM}} \simeq \frac{\Gamma(h \to \gamma\gamma)}{\Gamma(h \to \gamma\gamma)^{SM}}. \tag{23}$$

The new data of LHC presents the constraints on $R_{\gamma\gamma}$, $R_{\gamma\gamma} = 1.56 \pm 0.43$ for $m_h \simeq 125$ GeV from CMS [37] and $R_{\gamma\gamma} = 1.9 \pm 0.5$ for $m_h \simeq 126$ GeV from ATLAS [38].

By tuning the values of $\lambda_2$ and $\lambda_3$, $-3 \leq \lambda_1 \leq 10$ is allowed by the perturbative unitarity and stability of the potential [17]. Since the effects of $\lambda_2$ and $\lambda_3$ on $R_{\gamma\gamma}$ is suppressed by $v_t$, $R_{rr}$ is not sensitive to the choices of $\lambda_2$ and $\lambda_3$. We take $\lambda_4 = 0$, which leads that that $H^{\pm\pm}$ and $H^{\pm}$ have the same masses and couplings to $h$, which are proportional to $\lambda_1$. Therefore, $R_{\gamma\gamma}$ is only sensitive to the $m_{H^{\pm\pm}}$ and $\lambda_1$. Fig. 4 shows some contours for $R_{\gamma\gamma} = 1.2,\ 1.5,\ 2.0,\ 2.5$ in the plane of $\lambda_1$ versus $m_{H^{\pm\pm}}$. The $H^{\pm}$ and $H^{\pm\pm}$ contributions

are constructive with those of $W$ boson for $\lambda_1 < 0$, but destructively for $\lambda_1 > 0$. From Fig. 4, we can find that, if $\lambda_1$ is larger than 0, $1.2 < R_{\gamma\gamma} < 2.5$ requires $\lambda_1 > 4$ and $m_{H^{\pm\pm}} < 200$ GeV, which is similar to that of $SS \to \gamma\gamma$, namely a large coupling constant and the light charged scalars. For $\lambda_1 < 0$, the charged scalars masses can be larger than 300 GeV.

## VI. CONCLUSION

In the framework of Higgs triplet model, a real single scalar $S$ is introduced with a discrete $Z_2$ symmetry being imposed, which plays the role of the DM candidate. The interaction between DM and SM-like Higgs $h$ gives the dominant contributions to the total DM annihilation cross section and cross section of between DM and nucleon, which can make the model to satisfy the experimental constraints of DM relic density and direct detection data from Xenon100. The doubly charged scalar and one charged scalar can give the important contributions to the $SS \to \gamma\gamma$ annihilation and $h \to \gamma\gamma$ decay. For these charged scalars masses are suitable small, $< \sigma v >_{SS} \to \gamma\gamma$ can be enhanced to $\mathcal{O}(1) \times 10^{-27} cm^3 s^{-1}$, which gives a valid explanation for the claimed 130 GeV gamma-ray line signal. The LHC diphoton rate can be enhanced by a factor $1.2 \sim 2.5$, which fits the ATLAS and CMS data well. Besides, the model also predicts a 114 GeV gamma-ray line from the annihilation $SS \to \gamma Z$, whose cross section is below the upper bound reported by Fermi LAT.


### Acknowledgment

We thank Wen Long Sang, Wenyu Wang and Jin Min Yang for discussions. This work was supported by the National Natural Science Foundation of China (NNSFC) under grant Nos. 11005089 and 11105116.



[1] C. Weniger, JCAP **1208**, 007 (2012) [arXiv:1204.2797].

[2] T. Bringmann, X. Huang, A. Ibarra, S. Vogl, and C. Weniger, JCAP **1207**, 054 (2012) [arXiv:1203.1312]; E. Tempel, A. Hektor, and M. Raidal, arXiv:1205.1045.

[3] M. Su and D. P. Finkbeiner, arXiv:1206.1616.

[4] W. Atwood et al. (LAT Collaboration), Astrophys. J. 697, 1071 (2009) [arXiv:0902.1089].

[5] M. Su and D. P. Finkbeiner, arXiv:1207.7060.

[6] M. Ackermann et al. [Fermi-LAT Collaboration], Phys. Rev. D **86**, 022002 (2012) [arXiv:1205.2739].

[7] G. Jungman, M. Kamionkowski and K. Griest, Phys. Rept. **267**, 195 (1996) [hep-ph/9506380]; G. Bertone, D. Hooper and J. Silk, Phys. Rept. **405**, 279 (2005) [hep-ph/0404175].

[8] M. Ackermann et al. (Fermi-LAT collaboration), Phys. Rev. Lett. **107**, 241302 (2011) [arXiv:1108.3546].

[9] J. M. Cline, Phys. Rev. D **86**, 015016 (2012) [arXiv:1205.2688].

[10] M. R. Buckley and D. Hooper, Phys. Rev. D **86**, 043524 (2012) [arXiv:1205.6811].

[11] A. Ibarra, S. L. Gehler and M. Pato, JCAP **1207**, 043 (2012) [arXiv:1205.0007]; E. Dudas, Y. Mambrini, S. Pokorski and A. Romagnoni, arXiv:1205.1520; K. Y. Choi and O. Seto, Phys. Rev. D **86**, 043515 (2012) [arXiv:1205.3276]; H. M. Lee, M. Park and W. -I. Park, arXiv:1205.4675; A. Rajaraman, T. M. P. Tait and D. Whiteson, arXiv:1205.4723; B. S. Acharya, G. Kane, P. Kumar, R. Lu and B. Zheng, arXiv:1205.5789; X. Chu, T. Hambye, T. Scarna and M. H. G. Tytgat, arXiv:1206.2279; D. Das, U. Ellwanger and P. Mitropoulos, JCAP **1208**, 003 (2012) [arXiv:1206.2639]; Z. Kang, T. Li, J. Li and Y. Liu, arXiv:1206.2863; I. Oda, arXiv:1207.1537; R. -Z. Yang, Q. Yuan, L. Feng, Y. -Z. Fan and J. Chang, arXiv:1207.1621; L. Feng, Q. Yuan, Y.-Z, Fan, arXiv:1206.4758; B. Yang, J. Shelton, arXiv:1208.4100; L. Bergstrom, arXiv:1208.6028; J. M. Cline, A. R. Frey, G. D. Moore, arXiv:1208.2685; S. Tulin, H.-B. Yu, K. M. Zurek, arXiv:1208.0009; X.-Y. Huang, Q. Yuan, P.-F. Yin, X.-J. Bi, X.-L. Chen, arXiv:1208.0267; R. Laha, K. C. Yu Ng, B. Dasgupta, S, Horiuchi, arXiv:1208.5488; J. J. Fan, M. Reece, arXiv:1209.1097; J.-C. Park, S. C. Park, arXiv:1207.4981.

[12] V. Silveira, A. Zee, Phys. Lett. B **161**, (1985) 136.

[13] C. Bird, R. Kowalewski, M. Pospelov, Mod. Phys. Lett. A **21**, 457 (2006) [arXiv:hep-ph/0601090].

[14] K. Cheung, Y.-L. S. Tsai, P. Tseng, T. Yuan, A. Zee, arXiv:1207.4930.

[15] X.-G. He, B. Ren, J. Tandean, Phys. Rev. D **85**, 093019 (2012).

[16] W. Konetschny, W. Kummer, Phys. Lett. B **70**, 433 (1977); J. Schechter, J. W. F. Valle, Phys. Rev. D **22**, 2227 (1980); T. P. Cheng, L. F. Li, Phys. Rev. D **22**, 2860 (1980).

[17] A. G. Akeroyd, S. Moretti, Phys. Rev. D **86**, 035015 (2012) [arXiv:1206.0535].

[18] A. Arhrib, R. Benbrik, M. Chabab, G. Moultaka, L. Rahili, JHEP **1204**, 136 (2012).

[19] L. Wang, X.-F Han, arXiv:1206.1673.

[20] M. Carena, S. Gori, N. R. Shah, and C. E. M. Wagner, JHEP **1203**, 014 (2012); J. Cao, Z. Heng, D. Li, J. M. Yang, Phys. Lett. B **710**, 665-670 (2012); JHEP **1203**, 086 (2012); N. Christensen, T. Han, S. Su, Phys. Rev. D **85**, 115018 (2012) [arXiv:1203.3207]; L. Roszkowski, E. M. Sessolo, Y.-L. Sming Tsai, arXiv:1202.1503.

[21] J. F. Gunion, Y. Jiang, S. Kraml, Phys. Lett. B **710**, 454-459 (2012); U. Ellwanger, Phys. Lett. B **698**, 293 (2011); J. Cao, Z. Heng, T. Liu, J. M. Yang, Phys. Lett. B **703**, 462 (2011); D. A. Vasquez, G. Belanger, C. Boehm, J. Da Silva, P. Richardson, C. Wymant, Phys. Rev. D **86**, 035023 (2012) [arXiv:1203.3446]; F. King, M. Muhlleitner, R. Nevzorov, Nucl. Phys. B **860**, 207-244 (2012); J. Cao, Z. Heng, J. M. Yang, J. Zhu, arXiv:1207.3698; J. Ke, M.-X. Luo, L.-Y. Shan, K. Wang, L. Wang, arXiv:1207.0990.

[22] T. Li, X. Wan, Y.-K. Wang, S.-H. Zhu, arXiv:1203.5083; L. Wang, J. M. Yang, Phys. Rev. D **84**, 075024 (2011); A. Arhrib, R. Benbrik, N. Gaur, Phys. Rev. D **85**, 095021 (2012) [arXiv:1201.2644]; L. Wang, X.-F. Han, JHEP **1205**, 088 (2012); Y. Cai, W. Chao, S. Yang, arXiv:1208.3949; N. Chen, H.-J. He, JHEP **1204**, 062 (2012); M. R. Buckley, D. Hooper, arXiv:1207.1445; P. Giardino, K. Kannike, M. Raidal, A. Strumia, arXiv:1207.1347; S. Chang, C. A. Newby, N. Raj, C. Wanotayaroj, arXiv:1207.0493; T. Abe, N. Chen, H.-J. He, arXiv:1207.4103.

[23] E. Ma, M. Raidal and U. Sarkar, Phys. Rev. Lett. **85**, 3769 (2000); E. Ma, M. Raidal and U. Sarkar, Nucl. Phys. B **615**, 313 (2001); E. J. Chun, K. Y. Lee and S. C. Park, Phys. Lett. B **566**, 142 (2003).

[24] S. Kanemura, K. Yagyu, Phys. Rev. D **85**, 115009 (2012) [arXiv:1201.6287].

[25] CMS Collaboration, arXiv:1207.2666.

[26] A. G. Akeroyd and M. Aoki, Phys. Rev. D **72**, 035011 (2005).

[27] DELPHI Collaboration, J. Abdallah et al., Eur. Phys. Jour. C **34**, 399 (2004).

[28] K. Griest, D. Seckel, Phys. Rev. D **43**, 3191-3203 (1991).

[29] W.-L. Guo, Y.-L. Wu, JHEP **1010**, 083 (2010); R. N. Lerner, J. McDonald, Phys. Rev. D **80**, 123507 (2009); P. Burgess, M. Pospelov, T. Veldhuis, Nucl. Phys. B **619**, 709-728 (2001).

[30] E. Kolb and M. Turner, The Early Universe (Frontiers in Physics) (Westview Press, 1994).

[31] P. Gondolo and G. Gelmini, Nucl. Phys. B **360**, 145 (1991).

[32] E. Komatsu et al. [WMAP Collaboration], Astrophys. J. Suppl. **192**, 18 (2011).

[33] G. Jungman, M. Kamionkowski, K. Griest, Phys. Rept. **267**, 195 (1996); M. A. Shifman, A. I. Vainshtein and V. I. Zakharov, Phys. Lett. B **78**, 443 (1978).

[34] J. R. Ellis, K. A. Olive, Y. Santoso and V. C. Spanos, Phys. Rev. D **71**, 095007 (2005) [hep-ph/0502001].

[35] E. Aprile et al. [XENON100 Collaboration], Phys. Rev. Lett. **107**, 131302 (2011) [arXiv:1104.2549].

[36] A. Djouadi, Phys. Rept. **459**, 1 (2008).

[37] S. Chatrchyan et al. [CMS Collaboration], Phys. Lett. B **716**, 30-61 (2012) [arXiv:1207.7235].

[38] G. Aad et al. [ATLAS Collaboration], Phys. Lett. B **716**, 1-29 (2012) [arXiv:1207.7214].